Carrier-Induced Change in Refractive Index of InP, GaAs, and InGaAsP

BRIAN R. BENNETT, RICHARD A. SOREF, SENIOR MEMBER, IEEE, AND JESÚS A. DEL ALAMO, MEMBER, IEEE

Abstract—**We have theoretically estimated the change in refractive index Δn produced by injection of free carriers in InP, GaAs, and InGaAsP. Bandfilling (Burstein–Moss effect), band-gap shrinkage, and free-carrier absorption (plasma effect) were included. Carrier concentrations of $10^{16}/cm^3$ to $10^{19}/cm^3$ and photon energies of 0.8 to 2.0 eV were considered. Predictions of Δn are in reasonably good agreement with the limited experimental data available. Refractive index changes as large as 10^{-2} are predicted for carrier concentrations of $10^{18}/cm^3$, suggesting that low-loss optical phase modulators and switches using carrier injection are feasible in these materials.**

I. Introduction

GROUP III–V semiconductors are playing an increasingly important role in integrated optics because they offer the potential for integration of sources, detectors, switches, and modulators. Guided-wave switching and modulation can be achieved by perturbing the optical absorption coefficient and refractive index with an electric field [1]. Recently, Ishida *et al.* demonstrated free-carrier-induced optical switching in InGaAsP–InP [2], and Kowalsky and Ebeling achieved controlled transmission by optical injection in the same material system [3]. Mendoza-Alvarez *et al.* fabricated efficient GaAs–AlGaAs depletion-mode phase modulators in which both electric field and carrier effects were significant [4], [5]. Carrier-induced refractive index changes are also important for laser design [6] as well as new optical probing techniques for GaAs devices [7].

In this paper we estimate the carrier-induced changes in refractive index for InP, GaAs, and alloys of InGaAsP lattice-matched to InP. We consider the case of electrical or optical injection for carrier concentrations ranging from 10^{16} to $10^{19}/cm^3$. Three carrier effects: bandfilling, band-gap shrinkage, and free-carrier absorption, are included.

Manuscript received May 4, 1989; revised July 5, 1989. The work of B. R. Bennett was supported by an Air Force Office of Scientific Research Graduate Fellowship.

B. R. Bennett was with the Solid State Sciences Directorate, Rome Air Development Center, Hanscom Air Force Base, Bedford, MA 01731. He is now with the Department of Materials Science and Engineering, Massachusetts Institute of Technology, Cambridge, MA 02139.

R. A. Soref is with the Solid State Sciences Directorate, Rome Air Development Center, Hanscom Air Force Base, Bedford, MA 07131.

J. A. del Alamo is with the Department of Electrical Engineering and Computer Science, Massachusetts Institute of Technology, Cambridge, MA 02139.

IEEE Log Number 8931623.

II. Theory and Results

A. Bandfilling

A decrease in absorption for photon energies slightly above the nominal bandgap has been observed for several semiconductors when they are doped. The effect is most pronounced in semiconductors with small effective masses and energy gaps (e.g., n-InSb). This phenomenon, known as the Burstein–Moss effect, has been explained by bandfilling [8], [9]. In the case of n-type semiconductors, the density of states in the conduction band is sufficiently low that a relatively small number of electrons can fill the band to an appreciable depth. With the lowest energy states in the conduction band filled, electrons from the valence band require energies greater than the nominal bandgap to be optically excited into the conduction band (see Fig. 1). Hence, there is a decrease in the absorption coefficient at energies above the bandgap. The situation is similar for holes in p-type materials, but their larger effective mass means a higher density of states and hence a smaller bandfilling effect for a given carrier concentration. In this paper, we are interested in the effects of electron–hole plasmas that are injected into semiconductors by electrical or optical means. Since bandfilling is a result of free carriers, injection should be equivalent to doping, except that injection will result in bandfilling effects from both the electrons and holes.

If parabolic bands are assumed, the optical absorption near the bandgap in a direct-gap semiconductor is given by the square-root law:

$$\alpha_0(E) = \frac{C}{E}\sqrt{E - E_g} \qquad E \geq E_g$$

$$\alpha_0(E) = 0 \qquad E < E_g \tag{1}$$

where $E = \hbar\omega$ is the photon energy, E_g is the band-gap energy, and C is a constant involving materials parameters, matrix elements between periodic parts of the Bloch states at the band edges, and fundamental constants [9]. The valence bands in III–V semiconductors are degenerate at the direct gap (Γ-point in k-space), with both the light- and heavy-hole bands contributing to the absorption process (see Fig. 1). Equation (1) can be rewritten to explicitly consider the role of light and heavy holes in ab-

0018-9197/90/0100-0113$01.00 © 1990 IEEE

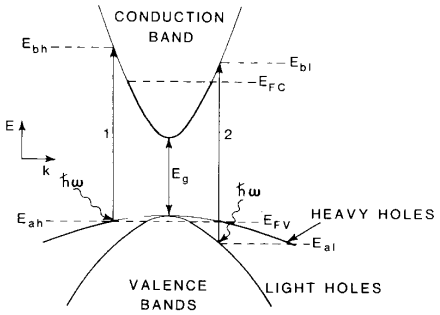

Fig. 1. Energy band structure and bandfilling effect for direct-gap semiconductor. Absorption of a photon can occur only between occupied valence band states and unoccupied conduction band states. Transitions involving heavy and light holes are denoted by 1 and 2, respectively.

TABLE I
VALUES OF SEMICONDUCTOR PARAMETERS (T = 300 K)

	InP	GaAs	$In_{0.82}Ga_{0.18}As_{0.40}P_{0.60}$
E_g(eV)	1.34	1.42	1.08
C($cm^{-1} \cdot s^{-1/2}$)	4.4×10^{12}	2.3×10^{12}	3.2×10^{12}
C_{hh}($cm^{-1} \cdot s^{-1/2}$)	2.8×10^{12}	1.5×10^{12}	2.1×10^{12}
C_{lh}($cm^{-1} \cdot s^{-1/2}$)	1.6×10^{12}	7.8×10^{11}	1.1×10^{12}
ϵ_s	12.4	13.1	13.0
n	3.4	3.6	3.6
$m_e(m_0)$	0.075	0.066	0.064
$m_{hh}(m_0)$	0.56	0.45	0.51
$m_{lh}(m_0)$	0.12	0.084	0.086
$m_{dh}(m_0)$	0.60	0.47	0.53
$\mu_{ehh}(m_0)$	0.066	0.058	0.057
$\mu_{elh}(m_0)$	0.046	0.037	0.037
N_c(cm^{-3})	5.2×10^{17}	4.3×10^{17}	4.1×10^{17}
N_v(cm^{-3})	1.2×10^{19}	8.3×10^{18}	1.1×10^{19}
χ_{cr}(cm^{-3})	1.3×10^{17}	7.4×10^{16}	7.0×10^{16}

sorption:

$$\alpha_0(E) = \frac{C_{hh}}{E}\sqrt{E - E_g} + \frac{C_{lh}}{E}\sqrt{E - E_g} \qquad E \geq E_g$$
$$\alpha_0(E) = 0 \qquad E < E_g \tag{2}$$

where C_{hh} and C_{lh} refer to heavy and light holes, respectively. The values of C for different materials were estimated by fitting (1) to experimental absorption data [10]. Then, C_{hh} and C_{lh} were calculated by using the fact that the concentrations of heavy and light holes are proportional to their effective masses to the three-halves power. For valence-to-conduction band absorption processes, the relevant parameters are the reduced effective masses of the electron–hole pairs [9] μ_{ehh} and μ_{elh}, which are given by

$$\mu_{ehh} = \left(\frac{1}{m_e} + \frac{1}{m_{hh}}\right)^{-1} \tag{3a}$$

$$\mu_{elh} = \left(\frac{1}{m_e} + \frac{1}{m_{lh}}\right)^{-1} \tag{3b}$$

where m_e, m_{hh}, and m_{lh} are the effective masses of electrons, heavy holes, and light holes, respectively. C_{hh} and C_{lh} are found from

$$C_{hh} = C\left(\frac{\mu_{ehh}^{3/2}}{\mu_{ehh}^{3/2} + \mu_{elh}^{3/2}}\right) \tag{4a}$$

$$C_{lh} = C\left(\frac{\mu_{elh}^{3/2}}{\mu_{ehh}^{3/2} + \mu_{elh}^{3/2}}\right). \tag{4b}$$

The values of C, C_{hh}, and C_{lh} are given in Table I. About two-thirds of the absorption results from heavy holes and one-third from light holes in all three materials.

In the case of bandfilling, there is a finite probability that a state in the conduction band will be occupied by an electron and/or a state in the valence band will be empty (of electrons). If we denote an energy in the valence band by E_a and an energy in the conduction band by E_b, then the absorption coefficient of an injected semiconductor is [11]

$$\alpha(N, P, E) = \alpha_0(E)\left[f_v(E_a) - f_c(E_b)\right] \tag{5}$$

where N and P are the concentrations of free electrons and holes, respectively, α_0 represents the absorption of pure materials in the absence of injection, $f_c(E_b)$ is the probability of a conduction band state of energy E_b being occupied by an electron, and $f_v(E_a)$ is the probability of a valence band state of energy E_a being occupied by an electron. For a given photon energy, the values of E_a and E_b are uniquely defined. Because of the degeneracy of the valence band, there will be two values for each (see Fig. 1). Applying energy and momentum conservation gives

$$E_{ah,al} = (E_g - E)\left(\frac{m_e}{m_e + m_{hh,lh}}\right) - E_g \tag{6a}$$

$$E_{bh,bl} = (E - E_g)\left(\frac{m_{hh,lh}}{m_e + m_{hh,lh}}\right) \tag{6b}$$

where the subscripts h and l refer to heavy and light holes, respectively.

The probabilities f_c and f_v in (5) are given by the Fermi–Dirac distribution functions

$$f_c(E_{bh,bl}) = \left[1 + e^{(E_{bh,bl} - E_{F_c})/(k_B T)}\right]^{-1} \tag{7a}$$

$$f_v(E_{ah,al}) = \left[1 + e^{(E_{ah,al} - E_{F_v})/(k_B T)}\right]^{-1} \tag{7b}$$

where k_B is Boltzmann's constant and T is absolute temperature. E_{F_c} and E_{F_v} are the carrier-dependent quasi-Fermi levels. We estimated them by the Nilsson approximation [12]

$$E_{F_c} = \left\{\ln\left(\frac{N}{N_c}\right) + \frac{N}{N_c}\left[64 + 0.05524\frac{N}{N_c} \cdot \left(64 + \sqrt{\frac{N}{N_c}}\right)\right]^{-(1/4)}\right\} k_B T \tag{8a}$$

$$E_{F_v} = \left(-\left\{ \ln\left(\frac{P}{N_v}\right) + \frac{P}{N_v}\left[64 + 0.05524\,\frac{P}{N_v} \cdot \left(64 + \sqrt{\frac{P}{N_v}} \right) \right]^{-(1/4)} \right\} - E_g \right) k_B T \qquad (8b)$$

where the zero of energy is defined to be at the conduction band minimum. In (8), N_c is the effective density of states in the conduction band

$$N_c = 2\left(\frac{m_e k_B T}{2\pi\hbar^2}\right)^{3/2} \qquad (9a)$$

and N_v is the effective density of states in the valence bands

$$N_v = 2\left(\frac{m_{dh} k_B T}{2\pi\hbar^2}\right)^{3/2} \qquad (9b)$$

where $m_{dh} = (m_{hh}^{3/2} + m_{lh}^{3/2})^{2/3}$ is the density-of-states effective mass for holes.

The bandfilling-induced change in absorption is

$$\Delta\alpha(N, P, E) = \alpha(N, P, E) - \alpha_0(E). \qquad (10)$$

Equation (10) gives the change in absorption produced by injection into a nominally undoped material. In the case of depletion of a doped semiconductor, the change in absorption will be the opposite of the $\Delta\alpha$ in (10): $\Delta\alpha(N, E) = \alpha_0(E) - \alpha(N, E)$ for an n-type semiconductor. Combining (2), (5), and (10)

$$\Delta\alpha(N, P, E) = \frac{C_{hh}}{E}\sqrt{E - E_g}\,[f_v(E_{ah}) - f_c(E_{bh}) - 1] + \frac{C_{lh}}{E}\sqrt{E - E_g}\,[f_v(E_{al}) - f_c(E_{bl}) - 1]. \qquad (11)$$

The only materials parameters required for (11) are the effective masses of electrons and holes, the energy gap, and the fitting constant C. These parameters, along with other important physical parameters such as N_c, are given in Table I. In the case of n-type semiconductors, f_v will nearly equal one, but f_c will be greater than zero for states near the bottom of the conduction band as a result of filling of the band with electrons. For p-type materials, f_c will be virtually zero, but f_v will be less than one near the top of the valence band due to the presence of holes. For the case of injection, we will have $f_c > 0$ and $f_v < 1$ close to the respective band edges. In all cases, (11) predicts $\Delta\alpha$ less than zero: bandfilling decreases the absorption coefficient at a fixed energy.

The real and imaginary parts of the refractive index $n + ik$ (or of the dielectric constant $\epsilon_1 + i\epsilon_2$) are not independent. They are related by the Kramers–Kronig integrals [13]. We are working with the absorption coefficient α rather than the extinction coefficient k; they are related by $\alpha = 4\pi k/\lambda$ where λ is the wavelength. The relationship between n and α is

$$n(E) = 1 + \frac{2c\hbar}{e^2} P \int_0^\infty \frac{\alpha(E')}{E'^2 - E^2}\,dE' \qquad (12)$$

where c is the speed of light, e is the electron charge, $E = \hbar\omega$ is the photon energy, and P indicates the principal value of the integral. Through (12), the refractive index can be calculated if the absorption coefficient is known for all frequencies ω. Hence, any change in the absorption coefficient $\Delta\alpha$ is accompanied by a change in the real refractive index Δn. In analogy with (10) we define

$$\Delta n(N, P, E) = n(N, P, E) - n_0(E) \qquad (13)$$

where n_0 is the refractive index of pure, uninjected material. The change in index is then given by

$$\Delta n(N, P, E) = \frac{2c\hbar}{e^2} P \int_0^\infty \frac{\Delta\alpha(N, P, E')}{E'^2 - E^2}\,dE'. \qquad (14)$$

Equation (11) was applied to InP for electron–hole injection levels ranging from 10^{16} to $10^{19}/\text{cm}^3$. Room temperature ($T = 300$ K) was used throughout this paper. We assumed that the semiconductor was nominally undoped ($< 10^{16}/\text{cm}^3$) so that the free-carrier density is entirely due to injection, and we assumed quasi-neutrality, implying $N = P$. The resulting $\Delta\alpha$'s are plotted in Fig. 2. The change in absorption begins at the bandgap [a result of our assumption of parabolic bands in (1)] and decreases for energies well above the gap. Maximum values of $\Delta\alpha$ range from 130 cm^{-1} for $10^{16}/\text{cm}^3$ to 3×10^4 cm^{-1} for $10^{19}/\text{cm}^3$.

The bandfilling (Burstein–Moss) effect is sometimes referred to as a shift of the absorption edge. A rigid-shift model is adequate for some applications, but (11) predicts a change in the shape of the α versus E curve, not a simple translation. In the case of very high carrier density where the quasi-Fermi levels are several $k_B T$ into the valence and conduction bands, the absorption coefficient will become very small near the bandgap and, depending on the sensitivity of the measurement, may result in an apparent shift of the edge. For example, a carrier concentration resulting in an electron Fermi level $5k_B T$ into the conduction band should decrease α by a factor of 150 near the bandgap.

The values of $\Delta\alpha$ from (11) were inserted into (14) and numerically integrated using Simpson's rule with a grid spacing of 1 meV. The decay in $\Delta\alpha$ for energies well above E_g (Fig. 2) is amplified by the denominator in the integral. Hence, only $\Delta\alpha$ within a few tenths of an electron-volt of E_g makes a significant contribution to Δn in the transparent regime. The results corresponding to Fig. 2, electron–hole injection in InP, are shown in Fig. 3. The refractive index decreases for energies near and below E_g, and Δn becomes positive for energies well above E_g. The perturbation of refractive index approaches zero for energies far above or below the bandgap.

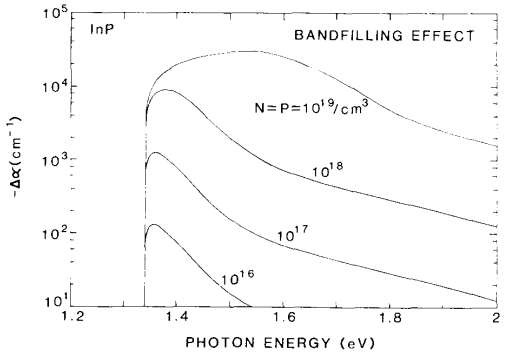

Fig. 2. Change in absorption due to electron-hole injection and the resulting bandfilling in InP [calculated from (11)].

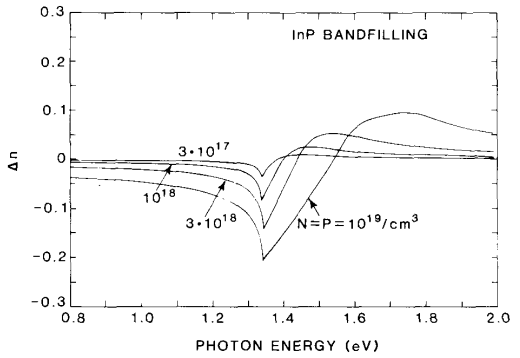

Fig. 3. Change in refractive index due to bandfilling in InP [calculated from (11) and (14)].

We would not expect to observe experimentally the sharp peaks in Δn near the bandgap predicted by the theory (Fig. 3). These features are a result of our assumption that the unperturbed absorption follows the square-root law, abruptly going to zero at E_g. In reality, materials exhibit absorption extending to energies below the nominal bandgap. This absorption tail, known as the Urbach edge, results from phonons, impurities, excitons, and internal electric fields [14]. The presence of this tail should not, however, have a significant effect on our estimation of Δn for energies substantially below the bandgap (i.e., $E < E_g - 0.1$ eV).

In Fig. 4 we plot the change in refractive index as a function of electron-hole pair density in InP for the fixed photon energies of 0.8, 1.0, and 1.2 eV, which are below the 1.34 eV bandgap. The effects are largest for energies close to E_g. Δn is linear in carrier concentration in the range 10^{16}–$10^{18}/\mathrm{cm}^3$ and can be expressed by

$$\Delta n(1.2\ \mathrm{eV}) \cong -1.4 \times 10^{-20}\chi$$
$$\Delta n(1.0\ \mathrm{eV}) \cong -7.7 \times 10^{-21}\chi$$
$$\Delta n(0.8\ \mathrm{eV}) \cong -5.6 \times 10^{-21}\chi \qquad (15)$$

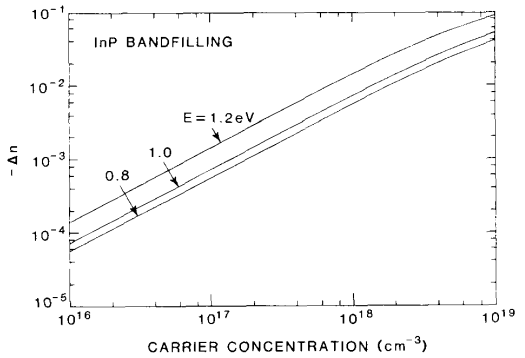

Fig. 4. Bandfilling-induced change in refractive index as a function of free-carrier concentration in InP. Quasi-neutrality is assumed: carrier concentration = $N = P$.

where $\chi = N = P$. Δn becomes sublinear for higher concentrations; (15) overestimates Δn by a factor of 1.5 at $\chi = 10^{19}/\mathrm{cm}^3$.

B. Bandgap Shrinkage

We will not attempt to review the considerable theoretical and experimental work on band-gap shrinkage (renormalization) effects in III–V semiconductors [15]–[23], but will present the relevant results. The basic mechanism is that injected electrons will occupy states at the bottom of the conduction band. If the concentration is large enough, the electron wave functions will overlap, forming a gas of interacting particles. The electrons will repel one another by Coulomb forces. In addition, electrons with the same spin will avoid one another for statistical reasons. The net result is a screening of electrons and a decrease in their energy, lowering the energy of the conduction band edge. A similar correlation effect for holes increases the energy of the valence band edge. The sum of these effects is band-gap shrinkage. Shrinkage effects are determined by free-carrier density, and are nearly independent of impurity concentration [24].

An expression for the band-gap shrinkage, originally derived by Wolff [15], is

$$\Delta E_g = -\left(\frac{e}{2\pi\epsilon_0\epsilon_s}\right)\left(\frac{3}{\pi}\right)^{1/3}\chi^{1/3} \qquad (16)$$

where χ is the concentration of free electrons or holes, ϵ_0 is the permittivity of free space, and ϵ_s is the relative static dielectric constant of the semiconductor. The estimated shrinkage is proportional to the cube-root of the carrier concentration or to the average interparticle spacing. Correlation effects become significant when the interelectron (hole) spacing becomes comparable in size to the effective Bohr radius of the electrons (holes). Hence, we do not expect the $\chi^{1/3}$ law to hold for low carrier concentrations because the carriers will be too far apart for significant

wave function overlap. We have adopted the model

$$\Delta E_g(\chi) = \frac{\kappa}{\epsilon_s}\left(1 - \frac{\chi}{\chi_{cr}}\right)^{1/3} \qquad \chi \geq \chi_{cr}$$

$$\Delta E_g(\chi) = 0 \qquad \chi < \chi_{cr} \qquad (17)$$

where κ is a fitting parameter and χ_{cr} is the critical concentration of free carriers. Equation (17) reduces to the predicted $\chi^{1/3}$ law for high carrier concentrations ($\chi >> \chi_{cr}$). Based upon experimental evidence [3], [18], [23], we have adopted a value of χ_{cr} equal to 1.4 times the Mott critical density [25]:

$$\chi_{cr} = 1.6 \times 10^{24}\left(\frac{m_e}{1.4\epsilon_s}\right)^3 \qquad (18)$$

with χ_{cr} in cm^{-3}. We use m_e rather than m_{hh} or m_{lh} in (18) for electron–hole plasmas because electron correlation effects begin at lower concentrations than hole effects. Equation (18) predicts $\chi_{cr} \cong 7 \times 10^{16}/cm^3$ for n-GaAs. which is in reasonable agreement with a recent estimate of $5 \times 10^{16}/cm^3$ [17].

Using (17) and adjusting κ, we were able to obtain good fits to published data for band-gap shrinkage in p-GaAs, n-GaAs, and injected electron–hole plasmas in GaAs; our estimates of κ are 0.11, 0.125, and 0.14, respectively. Because of the larger effective mass, χ_{cr} is larger for p-GaAs than for n-GaAs or electron–hole plasmas in GaAs. At fixed carrier concentrations, the predicted shrinkage is smallest for p-GaAs, a result of exchange coupling of light and heavy holes [16]. Fig. 5 shows the predictions of (17) and experimental data for n-GaAs and electron–hole plasmas in GaAs. The effects are slightly larger for electron–hole plasmas than for electrons of the same concentration, in agreement with theory [16]. There is very little data available for shrinkage in InP [23] and, to our knowledge, none for InGaAsP. Hence, we applied the values of κ calculated for GaAs to these materials, but the critical carrier density varied, depending upon the effective masses and dielectric constants.

We modeled the band-gap shrinkage to cause a rigid translation (red shift) of the absorption curve. The change in absorption due to shrinkage is predicted to be

$$\Delta\alpha(\chi, E) = \frac{C}{E}\sqrt{E - E_g - \Delta E_g(\chi)} - \frac{C}{E}\sqrt{E - E_g}. \qquad (19)$$

Equation (19) predicts $\Delta\alpha$ which is always positive, largest near the bandgap, and rapidly decreasing for higher energies. As with bandfilling, the change in refractive index was calculated by applying the Kramers–Kronig integral (14) to the $\Delta\alpha$ from (19). The results for InP with electron–hole carrier concentrations of 3×10^{17}, 10^{18}, and $3 \times 10^{18}/cm^3$ are given in Fig. 6. As in the case of bandfilling, the largest changes in refractive index are near the bandgap. Unlike bandfilling, however, Δn is positive for energies below the bandgap, a result of the increase in absorption coefficient for fixed energies.

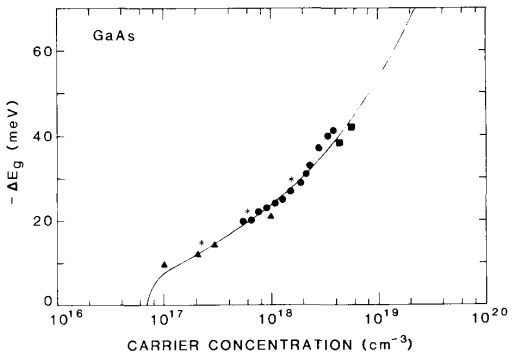

Fig. 5. Bandgap shrinkage in GaAs. Solid line is calculated from (17) with $\kappa = 0.13$ and $\chi_{cr} = 7 \times 10^{16}/cm^3$. Experimental points are for n-GaAs (▲ from [18] and ■ from [21]) and injected electron–hole pairs in GaAs (* from [19] and ● from [22]).

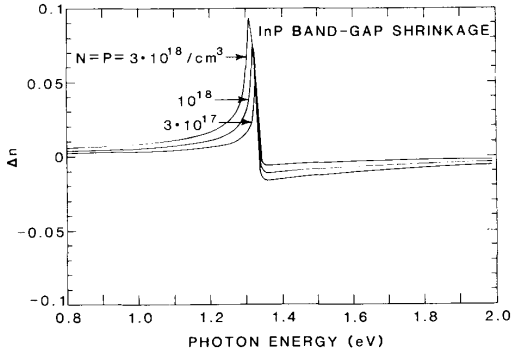

Fig. 6. Change in refractive index of InP due to electron–hole injection and the resulting band-gap shrinkage [calculated from (19) and (14)].

C. Free-Carrier Absorption

Thus far, we have considered changes of the interband absorption due to bandfilling and band-gap shrinkage effects. In addition, a free carrier can absorb a photon and move to a higher energy state within a band. In the Drude model, this intraband free-carrier absorption, also known as the plasma effect, is modeled as being directly proportional to the concentration of electrons and holes and the square of the wavelength. The corresponding change in refractive index is given by [26]

$$\Delta n = -\left(\frac{e^2\lambda^2}{8\pi^2c^2\epsilon_0 n}\right)\left(\frac{N}{m_e} + \frac{P}{m_h}\right) \qquad (20)$$

where λ is the photon wavelength. Unlike the bandfilling and band-gap shrinkage calculations, a numerical integration of absorption data is not necessary. Using the fact that the concentrations of heavy and light holes are proportional to their effective masses to the three-halves power, and inserting the values of fundamental constants

$$\Delta n = \frac{-6.9 \times 10^{-22}}{nE^2}\left\{\frac{N}{m_e} + P\left(\frac{m_{hh}^{1/2} + m_{lh}^{1/2}}{m_{hh}^{3/2} + m_{lh}^{3/2}}\right)\right\} \qquad (21)$$

with energy expressed in eV and N and P in cm^{-3}. For InP, the effective hole mass is $0.42m_0$ and the electron mass is $0.075m_0$. In the case of injection with equal concentrations of electrons and holes, the electron contribution to Δn will be about six times the hole contribution. Equation (21) is equivalent to the results derived by Stern [13] except that we use more recent estimates of effective mass. We are neglecting the change in refractive index due to intervalence band absorption. That effect is difficult to estimate, but is probably no more than 10 to 20 percent of the intraband Δn estimated by (21) [13].

The sign of Δn from the plasma effect is always negative; hence, it will add to bandfilling for energies below the bandgap. Because of the λ^2 dependence, the plasma effect increases as the photon energy is decreased below the bandgap. On the other hand, both the bandfilling and band-gap shrinkage effects on refractive index are largest near the bandgap and approach zero for $E << E_g$, as shown in Figs. 3 and 6.

D. Combination of Effects

The three carrier effects, bandfilling, band-gap shrinkage, and free-carrier absorption, were assumed to be independent. Hence, our estimate of the total change in refractive index is the simple sum of the effects. We did, however, estimate bandfilling based upon the shifted bandgap. That is, we modeled the injected free carriers as causing a contraction of the bandgap, followed by carrier filling of the new band structure. Experimental absorption data for InP [23] and GaAs [27] support this model.

The relative magnitudes of the three effects are illustrated in Fig. 7, which shows each effect and the total for electron–hole pairs in InP. A concentration of $3 \times 10^{16}/cm^3$ in Fig. 7(a) is below χ_{cr} (see Table I) and hence there is no shrinkage effect. The bandfilling and free-carrier effects are both negative below E_g. At $E = 0.95$ eV (1.3 μm) the bandfilling contribution is -0.00021 and the free-carrier contribution is -0.00012. At $3 \times 10^{17}/cm^3$ [Fig. 7(b)] the estimated shrinkage is 15 meV and the resulting positive Δn approximately cancels the Δn due to bandfilling and free-carrier absorption. The contributions to Δn ($E = 0.95$ eV) are: bandfilling -0.0021, shrinkage $+0.0030$, free-carrier absorption -0.0012, and total -0.0003. Finally, at $3 \times 10^{18}/cm^3$ [Fig. 7(c)] the shrinkage has increased to 39 meV, but the bandfilling-induced change in refractive index is clearly dominant, resulting in a net negative Δn at energies below the gap. At $E = 0.95$ eV the contributions to Δn are: bandfilling -0.019, shrinkage $+0.008$, free-carrier absorption -0.012, and total -0.023. The dominance of bandfilling over shrinkage for large χ is a result of the almost linear dependence of the bandfilling Δn on χ (Fig. 4) compared to the $\chi^{1/3}$ dependence of shrinkage. The largest values of Δn are found within a few meV of the bandgap, but the high absorption losses in the Urbach tail make waveguides and modulators impractical there.

Although our focus in this paper is estimating Δn for injection, we made calculations of the change in refractive index in n-InP and n-GaAs for comparison to experimental data on doping-induced index changes. Our procedures were basically the same as outlined above. For bandfilling, the only contribution is the filling of the conduction band with electrons and $f_v(E_a) = 1.0$ in (11). In Fig. 8 we show our predicted total Δn at 1.1 eV and experimental values [28]–[32] for n-InP at energies between 1.0 and 1.2 eV. For concentrations above $10^{18}/cm^3$, our model predicts bandfilling to be dominant, resulting in Δn

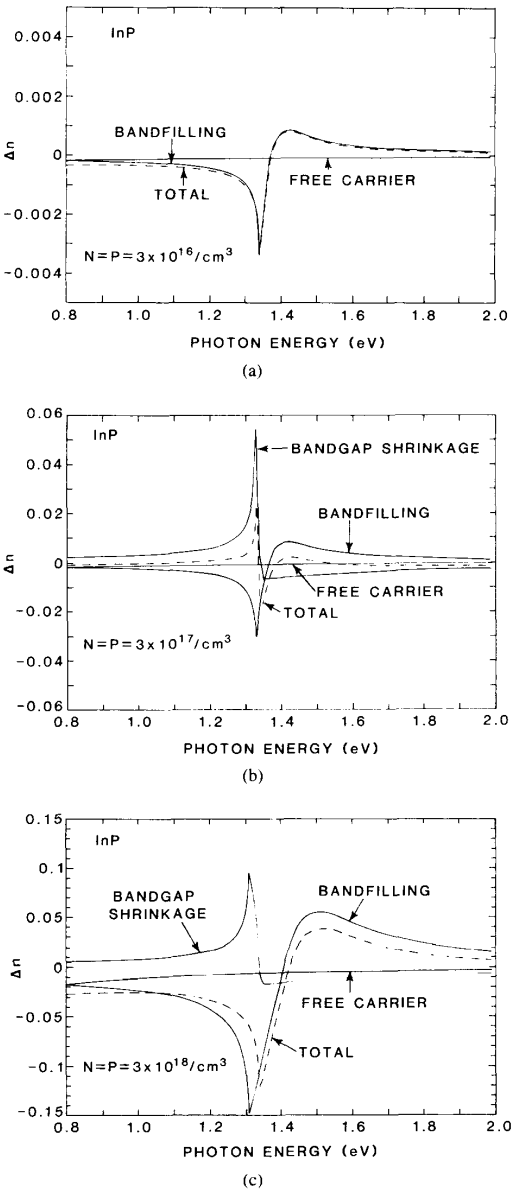

Fig. 7. Predicted changes in refractive index from bandfilling, band-gap shrinkage, and free-carrier absorption for injection into InP. (a) $N = P = 3 \times 10^{16}/cm^3$. (b) $N = P = 3 \times 10^{17}/cm^3$. (c) $N = P = 3 \times 10^{18}/cm^3$.

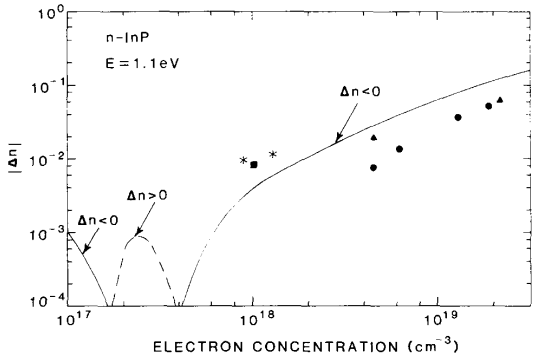

Fig. 8. Comparison of calculated and experimental Δn for n-InP. Solid and dotted lines are calculated (sum of all three effects at 1.1 eV). Experimental points are from the literature (at energies between 1.0 and 1.2 eV): • from [28], ▲ from [29], ■ from [30], and * from [31] and [32]. Δn is negative for all experimental points.

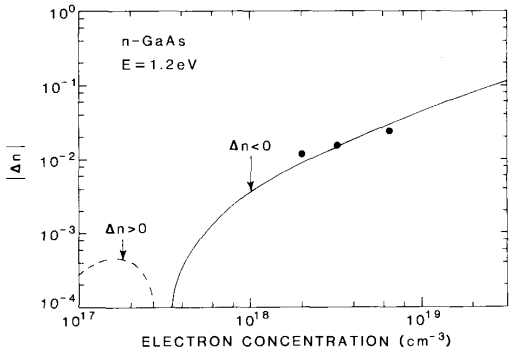

Fig. 9. Comparison of calculated and experimental Δn for n-GaAs at 1.2 eV. Solid and dotted lines are calculated (sum of all three effects). Experimental points are from [33]. Δn is negative for all experimental points.

< 0. The experimental Δn's are also negative, supporting our model. Results for GaAs (Fig. 9) show excellent agreement with experimental data [33]. We also compared our predicted results to estimates of Δn which Zoroofchi and Butler [34] obtained by applying Kramers–Kronig integrals to GaAs experimental absorption data. At $E = 1.37$ eV and $N = 1.2 \times 10^{18}/\text{cm}^3$, we predict $\Delta n = -0.0070$ and their value is -0.0066. At $E = 1.37$ eV and $N = 6.5 \times 10^{18}/\text{cm}^3$, we predict $\Delta n = -0.045$ and their value is -0.046.

In Fig. 10 we plot the total estimated change in refractive index for InP as a function of carrier concentration ($\chi = N = P$) for two wavelengths in the transparent region, 1.3 and 1.55 μm. For carrier concentrations less than about $10^{17}/\text{cm}^3$, the interparticle spacing is too large for shrinkage effects (i.e., $\chi < \chi_{cr}$) and bandfilling dominates, yielding a negative Δn. Band-gap shrinkage effects are important over the range $10^{17} \leq \chi \leq 5 \times 10^{17}/\text{cm}^3$, approximately canceling the bandfilling and plasma terms at 1.3 μm. For higher carrier concentrations, bandfilling and plasma effects dominate, yielding a large negative Δn. Estimates of the total Δn for GaAs (same photon energies) are shown in Fig. 11. The results are similar, but the values of Δn are generally smaller than for InP because the 0.95 and 0.8 eV energies are farther from the GaAs bandgap. We note that the results in Figs. 10 and 11 for the 8×10^{16} to $5 \times 10^{17}/\text{cm}^3$ range are very sensitive to the value of χ_{cr}.

We also estimated Δn for electron–hole plasmas in InAs ($E_g = 0.36$ eV). Free-carrier absorption dominates for $\chi \geq 10^{17}/\text{cm}^3$. From (21), using $n = 3.6$, $m_e = 0.023$, $m_{hh} = 0.41$, and $m_{lh} = 0.025$, we obtain $\Delta n \cong -1.5 \times 10^{-19}\, \chi$ at $E = 0.24$ eV (5 μm). This yields -0.015 and -0.15 at 10^{17} and $10^{18}/\text{cm}^3$, respectively.

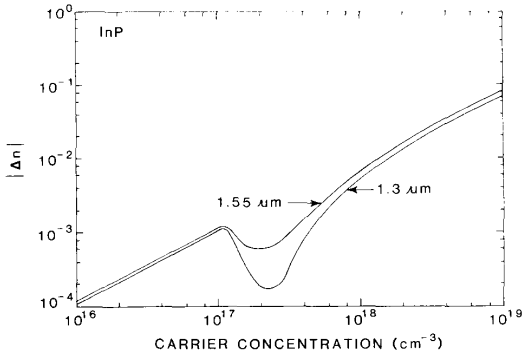

Fig. 10. Change in refractive index at 1.3 μm (0.95 eV) and 1.55 μm (0.8 eV) for carrier injection in InP. All three effects are included and $N = P$ is assumed. The sign of Δn is negative in all cases.

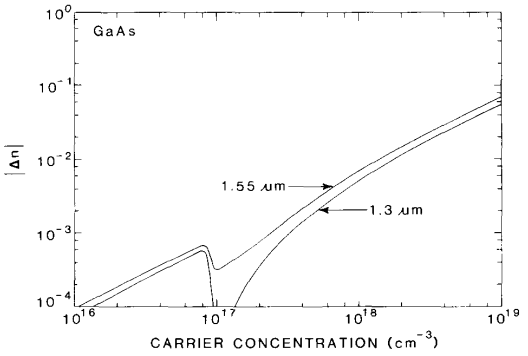

Fig. 11. Change in refractive index at 1.3 μm (0.95 eV) and 1.55 μm (0.8 eV) for carrier injection in GaAs. All three effects are included and $N = P$ is assumed. The sign of Δn is negative in all cases.

E. InGaAsP Alloys

Alloys of InGaAsP are the material of choice for lasers in "long-wave" optical communications systems. The degrees of freedom provided by the quaternary system allow lattice matching to InP with energy gaps ranging from 0.75 to 1.35 eV. This range includes the minimum loss (1.55 μm) and minimum dispersion (1.3 μm) wavelengths for silica optical fibers. Recently, optical wave-

guides and electrooptical switches have been fabricated in InP and InGaAsP [1], [2].

Alloys of $In_{1-x}Ga_xAs_yP_{1-y}$ are lattice-matched to InP when $y \cong 2.2x$. The experimental band-gap energy has been fit by [35]

$$E_g = 1.35 - 0.72y + 0.12y^2. \quad (22)$$

We applied our previous equations for bandfilling, band-gap shrinkage, and plasma effects to estimate Δn for injection of electron–hole plasmas in InGaAsP. The required parameters were energy gap, effective masses of electrons and holes, refractive index, static dielectric constant, and the absorption fitting parameter C in (1). We used (22) for the energy gap, and experimental values of electron and light-hole effective mass from Pearsall [35]. For heavy holes, we assumed a linear relationship varying from 0.41 for $In_{0.53}Ga_{0.47}As$ to 0.56 for InP. We note, however, that reported experimental values of m_{hh} for InP vary from 0.40 to 0.85. The refractive index for energies near the bandgap is nearly constant; we adopted a value of 3.6 for all compositions [36]. We used the fit by Adachi [36] for the static dielectric constant:

$$\epsilon_s(y) = 12.40 + 1.5y. \quad (23)$$

To estimate C, we used the fact that theoretically C should be proportional to the reduced effective mass to the three-halves power [9], and scaled accordingly from the value for InP [10]. The parameters are included in Table I.

An advantage of using InGaAsP is that the energy gap can be adjusted to maximize Δn for a given wavelength. We could choose a bandgap close enough to the operating wavelength to obtain a large Δn (see Fig. 7) but not so close that absorption losses are prohibitive. For Fig. 12 we have chosen a bandgap of 1.08 eV, yielding a composition of $In_{0.82}Ga_{0.18}As_{0.40}P_{0.60}$. This bandgap is substantially closer than the bandgaps of InP and GaAs to the important 1.3 and 1.55 μm wavelengths, and the predicted Δn's are larger. The promixity of the bandgap also results in $\Delta n > 0$ in the 10^{17}–$3 \times 10^{17}/cm^3$ range.

F. Phase Modulators

To illustrate the application of carrier effects to electrooptical phase modulators, we calculate L_π, the modulator length required to attain π radians of phase shift, which is given by

$$L_\pi = \frac{\lambda}{2|\Delta n|}. \quad (24)$$

In Fig. 13 we show L_π as a function of carrier concentration for InP and $In_{0.82}Ga_{0.18}As_{0.40}P_{0.60}$ at 1.3 μm. The increases in L_π in the 8×10^{16}–$5 \times 10^{17}/cm^3$ range result from band-gap shrinkage effects opposing the bandfilling and plasma effects. The values of L_π for InP range from 6 mm at $10^{16}/cm^3$ to 9 μm at $10^{19}/cm^3$. Predictions of the Franz–Keldysh effect at the same wavelength [37] yield much larger L_π's: 50 mm at a field strength of 10^5 V/cm and 800 μm at 6×10^5 V/cm, the breakdown

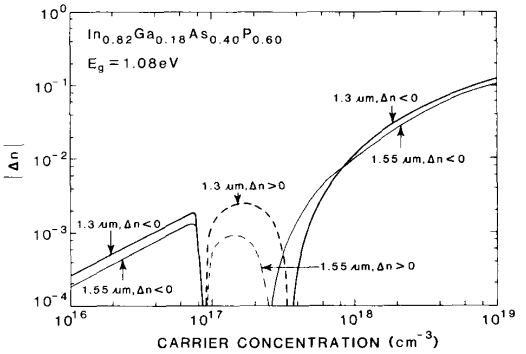

Fig. 12. Change in refractive index at 1.3 μm (0.95 eV) and 1.55 μm (0.8 eV) for carrier injection in $In_{0.82}Ga_{0.18}As_{0.40}P_{0.60}$. All three effects are included and $N = P$ is assumed. Solid lines represent $\Delta n < 0$ and dotted lines represent $\Delta n > 0$.

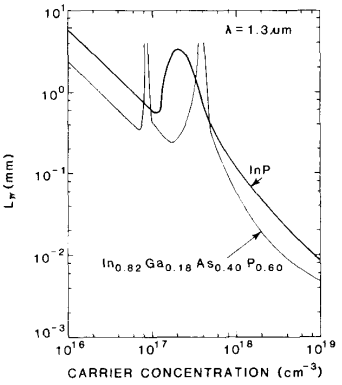

Fig. 13. Waveguide length required for 180° phase shift in InP and InGaAsP modulators at 1.3 μm (calculated from (24) and Figs. 10 and 12). The singularities for InGaAsP at 9×10^{16} and $4 \times 10^{17}/cm^3$ result from a change in the sign of Δn.

field strength of InP. The estimates of L_π for $In_{0.82}Ga_{0.18}As_{0.40}P_{0.60}$ are generally a factor of 1.5 to 2.5 smaller than the InP values, reflecting the fact that the InGaAsP bandgap is closer to the 1.3 μm wavelength.

In addition to the magnitude of the index change, optical absorption losses should be considered in the design of phase modulators. The bandfilling effect decreases absorption for energies near the bandgap. Band-gap shrinkage increases absorption, but the effect does not extend to energies below the new bandgap. Free-carrier absorption, however, increases as λ^2 [9] and dominates the loss at energies below the bandgap. The total optical insertion loss of a phase modulator in dB is given by $10 \log_{10} [\exp(\alpha L_\pi)]$. For $In_{0.82}Ga_{0.18}As_{0.40}P_{0.60}$ at $2 \times 10^{16}/cm^3$, we have $L_\pi \cong 1.2$ mm from Fig. 13, and $\alpha \cong 0.035\ cm^{-1}$ from [38], yielding a loss of only 0.02 dB. At $10^{18}/cm^3$, the absorption coefficient is much higher, about 2 cm^{-1}, but larger changes in refractive index mean a smaller L_π, 0.06 mm, and the predicted loss, 0.05 dB, is still very small.

III. Discussion

Our analysis shows that all three carrier effects can give substantial contributions to the refractive index near the direct-gap of III–V semiconductors. Precise estimates of the effects are limited by uncertainties in fundamental parameters such as effective masses and the lack of experimental data for band-gap shrinkage near $10^{17}/\text{cm}^3$. Despite these uncertainties, we believe that our estimates should generally be valid to within a factor of two. Although there are no direct experimental measurements of Δn over the wide range of carrier concentrations investigated here, we can test the validity of our results by comparison to some experimental data. Our model predicts Δn's comparable to those measured in InGaAsP and AlGaAs lasers by Manning *et al.* [5]. They pointed out that plasma effects alone are too small to account for the observed Δn's. Our analysis suggests that bandfilling is dominant over shrinkage effects for the carrier concentrations studied, $2\text{–}5 \times 10^{18}/\text{cm}^3$. We tested our model at lower concentrations by comparing our predicted $\Delta\alpha$'s to the changes in transmission of InGaAsP at 1.3 μm, measured by Kowalsky and Ebeling [3] for optical excitation with concentrations up to $5 \times 10^{16}/\text{cm}^3$. Our predictions agree with their data to within about 10 percent. We also predict $\Delta n = -0.002$ at 1.55 μm (0.15 eV below the bandgap) for $N = P = 5 \times 10^{16}/\text{cm}^3$, suggesting that their device structure could also be used as a phase modulator.

Our results should also approximately apply to depletion of doped semiconductors since the effects are, to first order, independent of impurities. The density of states in heavily-doped semiconductors exhibit band-tailing which we did not explicitly consider, but the agreement with experimental data in Figs. 8 and 9 indicates that our model is a good approximation. Our analysis suggests that shrinkage effects may have been important in the depletion-edge modulators of Mendoza-Alvarez *et al.* [4], [5] for n-GaAs with $N = 1\text{–}5 \times 10^{17}/\text{cm}^3$. The shrinkage would give a contribution to Δn opposing the bandfilling, plasma, and electric field effects.

Our results show a competition between bandfilling and band-gap shrinkage effects for carrier concentrations greater than the critical density χ_{cr}. Beyond about $10^{18}/\text{cm}^3$, bandfilling dominates resulting in $\Delta n < 0$. Bugajski and Lewandowski report a transition in the peak position of the InP photoluminescence spectra at the same carrier concentrations [23].

Injection levels of about $10^{18}/\text{cm}^3$ are practical in III–V devices. At that level, the predicted index changes are as large as 10^{-2} which is substantially larger than the Δn produced by the Pockels or Franz–Keldysh effects at a field strength of 10^5 V/cm [10]. Recent studies have also considered the use of multiple quantum wells to achieve enhanced electric field and carrier-induced refractive index changes, with estimates of Δn as large as 10^{-2} to 10^{-1} [39], [40].

IV. Summary and Conclusions

We have estimated carrier-induced changes in the refractive index of InP, GaAs, and InGaAsP. Three effects, bandfilling, band-gap shrinkage, and free-carrier absorption, can produce substantial contributions to the total Δn. The bandfilling and free-carrier absorption effects both produce a negative Δn for wavelengths in the transparent regime of the semiconductors; band-gap shrinkage produces a positive Δn in the same regime. Our models give reasonable agreement with experimental data for doped semiconductors and predict substantial changes in refractive index over a wide range of injected carrier concentrations. The effects can be enhanced by employing alloys such as InGaAsP and by adjusting the bandgap to be near the desired wavelength. These results suggest that low-loss optical switches and phase modulators based upon carrier injection are feasible in direct-gap III–V compound semiconductors.

Acknowledgment

The authors thank D. R. Greenberg, J. P. Lorenzo, K. Vaccaro, and A. C. Yang for technical discussions.

References

[1] J. P. Donnelly, N. L. DeMeo, F. L. Leonberger, S. H. Groves, P. Vohl, and F. J. O'Donnell, "Single-mode optical waveguides and phase modulators in the InP material system," *IEEE J. Quantum Electron.*, vol. QE-21, pp. 1147–1151, 1985.

[2] K. Ishida, H. Nakamura, H. Matsumura, T. Kadoi, and H. Inoue, "InGaAsP/InP optical switches using carrier induced refractive index change," *Appl. Phys. Lett.*, vol. 50, pp. 141–142, 1987.

[3] W. Kowalsky and K. J. Ebeling, "Optically controlled transmission of InGaAsP epilayers," *Opt. Lett.*, vol. 12, pp. 1053–1055, 1987.

[4] J. G. Mendoza-Alvarez, R. H. Yan, and L. A. Coldren, "Contribution of the band-filling effect to the effective refractive-index change in double-heterostructure GaAs/AlGaAs phase modulators," *J. Appl. Phys.*, vol. 62, pp. 4548–4553, 1987.

[5] J. G. Mendoza-Alvarez, L. A. Coldren, A. Alping, R. H. Yan, T. Hausken, K. Lee, and K. Pedrotti, "Analysis of depletion edge translation lightwave modulators," *J. Lightwave Technol.*, vol. 6, pp. 793–808, 1988.

[6] J. Manning, R. Olshansky, and C. B. Su, "The carrier-induced index change in AlGaAs and 1.3 μm InGaAsP diode lasers," *IEEE J. Quantum Electron.*, vol. QE-19, pp. 1525–1530, 1983.

[7] G. N. Koskowich and M. Soma, "Voltage measurement in GaAs Schottky barriers using optical phase modulation," *IEEE Electron Device Lett.*, vol. 9, pp. 433–435, 1988.

[8] E. Burstein, "Anomalous optical absorption limit in InSb," *Phys. Rev.*, vol. 93, pp. 632–633, 1954.

[9] T. S. Moss, G. J. Burrell, and B. Ellis, *Semiconductor Opto-electronics*. New York: Wiley, 1973, pp. 48–94.

[10] B. R. Bennett and R. A. Soref, "Electrorefraction and electroabsorption in InP, GaAs, GaSb, InAs, and InSb," *IEEE J. Quantum Electron.*, vol. QE-23, pp. 2159–2166, 1987.

[11] A. Yariv, *Optical Electronics*, 3rd ed. New York: Holt, Rinehart and Winston, 1985, pp. 474–478.

[12] N. G. Nilsson, "Empirical approximations for the Fermi energy in a semiconductor with parabolic bands," *Appl. Phys. Lett.*, vol. 33, pp. 653–654, 1978.

[13] F. Stern, "Dispersion of the index of refraction near the absorption edge of semiconductors," *Phys. Rev. A*, vol. 133, pp. 1653–1664, 1964.

[14] J. D. Dow and D. Redfield, "Toward a unified theory of Urbach's rule and exponential absorption edges," *Phys. Rev. B*, vol. 5, pp. 594–610, 1972.

[15] P. A. Wolff, "Theory of the band structure of very degenerate semiconductors," *Phys. Rev.*, vol. 126, pp. 405-412, 1962.
[16] R. A. Abram, G. N. Childs, and P. A. Saunderson, "Band gap narrowing due to many-body effects in silicon and gallium arsenide," *J. Phys. C: Solid State Phys.*, vol. 17, pp. 6105-6125, 1984.
[17] H. S. Bennett and J. R. Lowney, "Models for heavy doping effects in gallium arsenide," *J. Appl. Phys.*, vol. 62, pp. 521-527, 1987.
[18] J. A. Rossi, D. L. Keune, N. Holonyak, Jr., P. D. Dapkus, and R. D. Burnham, "Threshold requirements and carrier interaction effects in GaAs platelet lasers (77°K)," *J. Appl. Phys.*, vol. 41, pp. 312-320, 1970.
[19] J. Camassel, D. Auvergne, and H. Mathieu, "Temperature dependence of the band gap and comparison with the threshold frequency of pure GaAs lasers," *J. Appl. Phys.*, vol. 46, pp. 2683-2689, 1975.
[20] H. C. Casey Jr. and F. Stern, "Concentration-dependent absorption and spontaneous emission of heavily doped GaAs," *J. Appl. Phys.*, vol. 47, pp. 631-643, 1976.
[21] M. Druminski, H.-D. Wolf, K.-H. Zschauer, and K. Wittmaack, "Unexpectedly high energy photoluminescence of highly Si doped GaAs grown by MOVPE," *J. Cryst. Growth*, vol. 57, pp. 318-324, 1982.
[22] S. Tarucha, H. Kobayashi, Y. Horikoshi, and H. Okamoto, "Carrier-induced energy-gap shrinkage in current-injection GaAs/AlGaAs MQW heterostructures," *Japan. J. Appl. Phys.*, vol. 23, pp. 874-878, 1984.
[23] M. Bugajski and W. Lewandowski, "Concentration-dependent absorption and photoluminescence of n-type InP," *J. Appl. Phys.*, vol. 57, pp. 521-530, 1985.
[24] L. P. Zverev, S. A. Negashev, V. V. Kruzhaev, and G. M. Min'kov, "Mechanism of band gap variation in heavily doped gallium arsenide," *Sov. Phys.—Semicond.*, vol. 11, pp. 603-605, 1977.
[25] K.-F. Berggren and B. E. Sernelius, "Band-gap narrowing in heavily doped many-valley semiconductors," *Phys. Rev. B*, vol. 24, pp. 1971-1986, 1981.
[26] C. H. Henry, R. A. Logan, and K. A. Bertness, "Spectral dependence of the change in refractive index due to carrier injection in GaAs lasers," *J. Appl. Phys.*, vol. 52, pp. 4457-4461, 1981.
[27] H. C. Casey Jr., D. D. Sell, and K. W. Wecht, "Concentration dependence of the absorption coefficient for n- and p-type GaAs between 1.3 and 1.6 eV," *J. Appl. Phys.*, vol. 46, pp. 250-257, 1975.
[28] M. S. Whalen and J. Stone, "Index of refraction of n-type InP at 0.633-μm and 1.15-μm wavelengths as a function of carrier concentration," *J. Appl. Phys.*, vol. 53, pp. 4340-4343, 1982.
[29] J. Stone and M. S. Whalen, "Index of refraction dispersion of n- and p-type InP between 0.95 and 2.0 eV," *Appl. Phys. Lett.*, vol. 41, pp. 1140-1142, 1982.
[30] A. D. Yas'kov, "Influence of doping on the dispersion of the optical refractive index of semiconductors," *Sov. Phys.—Semicond.*, vol. 17, pp. 937-939, 1983.
[31] V. B. Bogdanov, V. T. Prokopenko, and A. D. Yas'kov, "Effect of doping on the refractive index of indium phosphide in the region of the intrinsic absorption edge," *Opt. Spectrosc. (USSR)*, vol. 62, pp. 551-552, 1987.
[32] A. N. Pikhtin and A. D. Yas'kov, "Refraction of light in semiconductors (review)," *Sov. Phys.—Semicond.*, vol. 22, pp. 613-626, 1988.
[33] D. D. Sell, H. C. Casey, Jr., and K. W. Wecht, "Concentration dependence of the refractive index for n- and p-type GaAs between 1.2 and 1.8 eV," *J. Appl. Phys.*, vol. 45, pp. 2650-2657, 1974.
[34] Z. Zoroofchi and J. K. Butler, "Refractive index of n-type gallium arsenide," *J. Appl. Phys.*, vol. 44, pp. 3697-3699, 1973.
[35] T. P. Pearsall, Ed., *GaInAsP Alloy Semiconductors*. New York: Wiley, 1982.
[36] S. Adachi, "Material parameters of $In_{1-x}Ga_xAs_yP_{1-y}$ and related binaries," *J. Appl. Phys.*, vol. 53, pp. 8775-8792, 1982.
[37] B. R. Bennett and R. A. Soref, "Analysis of Franz-Keldysh electrooptic modulation in InP, GaAs, GaSb, InAs, and InSb," *Proc. SPIE*, vol. 836, Optoelectron. Materials, Devices, Packaging, Interconnects, pp. 158-168, 1988.
[38] F. Fiedler and A. Schlachetzki, "Optical parameters of InP-based waveguides," *Solid-State Electron.*, vol. 30, pp. 73-83, 1987.
[39] D. S. Chemla, I. Bar-Joseph, J. M. Kuo, T. Y. Chang, C. Klingshirn, G. Livescu, and D. A. B. Miller, "Modulation of absorption in field-effect quantum well structures," *IEEE J. Quantum Electron.*, vol. 24, pp. 1664-1676, 1988.
[40] U. Koren, T. L. Koch, B. I. Miller, and A. Shahar, "InGaAs/InGaAsP distributed feedback quantum well laser with an intracavity phase modulator," *Appl. Phys. Lett.*, vol. 53, pp. 2132-2134, 1988.

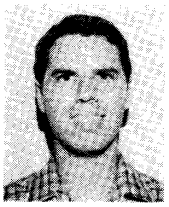

Brian R. Bennett was born in Kansas in 1962. He received the B.S. and M.S. degrees in 1984 and 1985, respectively, from the Massachusetts Institute of Technology, Cambridge, where he held both research and teaching assistantships. His M.S. thesis investigated the conductivity of the earth's crust and upper mantle using simultaneous measurements of electric and magnetic fields.

He served in the Air Force's Solid State Sciences Directorate at Hanscom Air Force Base, Bedford, MA, from 1984 to 1988. His research work included low-temperature deposition of silicon dioxide and electrooptic effects in III-V semiconductors. He is currently pursuing the Ph.D. degree in electronic materials at M.I.T. on an Air Force Office of Scientific Research Fellowship.

Mr. Bennett is a member of the Materials Research Society, the Electrochemical Society, the Society for Optical Engineering, the American Physical Society, and Sigma Xi.

Richard A. Soref (S'58-M'63-SM'71) received the B.S.E.E. and M.S.E.E. degrees from the University of Wisconsin and the Ph.D. degree in electrical engineering from Stanford University, Stanford, CA, in 1958, 1959, and 1963, respectively.

From 1963 to 1965, he was with the optics and infrared group of the Massachusetts Institute of Technology Lincoln Laboratory, Lexington, MA, and in 1965 he joined the Technical Staff of the Sperry Research Center, Sudbury, MA, where he conducted research on nonlinear optics, extrinsic silicon infrared detectors, liquid crystal electrooptic devices, optical switching, and fiber-optic sensors. In November 1983, he joined the Rome Air Development Center, Hanscom AFB, Bedford, MA, as a Research Scientist in the Solid State Sciences Directorate. His current interests include silicon and III-V integrated optics. He has authored or coauthored about 85 journal articles and holds 28 patents.

Dr. Soref is a member of the American Physical Society, the Society of Photo-Optical Instrumentation Engineers, and the Optical Society of America. He has served as Chairman of the Boston Chapter of the IEEE Electron Device Society and as an Editorial Advisor of the journal *Optical Engineering*. In 1988 he received the Charles E. Ryan Memorial Award for basic research on electrooptic guided-wave technology from the Rome Air Development Center, Hanscom AFB.

Jesús A. del Alamo (S'79-M'85) was born in Soria, Spain, in 1957. He received the Telecommun. Eng. degree from the Polytechnic University of Madrid, Madrid, Spain, in 1980, and the M.S. and Ph.D. degrees in electrical engineering from Stanford University, Stanford, CA, in 1983 and 1985, respectively.

From 1977 to 1981 he was research assistant with the Institute of Solar Energy of the Polytechnic University of Madrid, working on silicon solar cells. At Stanford University he carried out his Ph.D. dissertation on minority carrier transport in heavily-doped silicon and its relevance to bipolar transistors and solar cells. From 1985 to 1988 he was a research engineer with the Nippon Telegraph and Telephone Corp., at the NTT LSI Laboratories, Atsugi, Japan. He conducted research on heterostructure field-effect transistors based on InP, InAlAs, and InGaAs fabricated by molecular-beam epitaxy. He is presently an Assistant Professor with the Department of Electrical Engineering and Computer Science, Massachusetts Institute of Technology, Cambridge, where he is continuing research on heterostructure devices based on compound semiconductors.

Dr. del Alamo is a member of the Materials Research Society, the American Physical Society, and the Japanese Society of Applied Physics. He received the First Prize in the 1980 IEEE Region VIII Undergraduate Student Paper Contest and an Electrochemical Society Research Summer Fellowship Award in 1983. He was a Vinton Hayes Fellow at M.I.T. during 1988.